Journal of The Electrochemical Society, **159** (4) K107-K109 (2012)
0013-4651/2012/159(4)/K107/3/$28.00 © The Electrochemical Society

Carboxylic Group as the Origin of Electrical Performance Degradation during the Transfer Process of CVD Growth Graphene

Seul Ki Hong, Seung Min Song, Onejae Sul, and Byung Jin Cho[z]

Department of Electrical Engineering, KAIST, Daejeon 305-701, Korea

The large synthesis of graphene films by chemical vapor deposition (CVD) is expected to enable various applications. However, the transfer process of graphene from metal to dielectric substrate becomes a practical limitation in CVD method because of various chemical and mechanical stresses. In this paper, we have studied the critical factor of degradation and thereby to improve the electrical performance of graphene by CVD. It has been found that O=C–OH bonding is related to mobility degradation and doping effect. The removal of O=C–OH improves the carrier mobility by 30%.
© 2012 The Electrochemical Society. [DOI: 10.1149/2.101204jes] All rights reserved.

Manuscript submitted December 5, 2011; revised manuscript received January 20, 2012. Published February 9, 2012.

Graphene, a two-dimensional monolayer of sp^2-bonded carbon atoms, has been intensively studied due to its useful electrical and mechanical properties, including extremely high mobility, high elasticity, and electromechanical modulation.[1–4] Since the discovery of graphene prepared by mechanical exfoliation, many electrical and chemical approaches to synthesize large-scale graphene have been developed. Recent advances in large-area synthesis of graphene films by chemical vapor deposition (CVD) on Cu or Ni substrates[5–9] are expected to enable various macroscopic applications such as graphene FETs on a wafer scale and transparent conducting films for flexible/stretchable electronics. However, the transfer[10] of graphene grown via CVD from a seed metal to a dielectric presents a practical limitation in such applications, because various chemical and mechanical damages to graphene layers are unavoidable during this step. In this work, we have carefully studied each transfer step to identify the critical factors on electronic performance degradation and thereby improve the performance of graphene.

Experimental

We grew a large-scale graphene layer on a Cu substrate inside a CVD chamber, because the low solubility of the metal prevents stacking of multiple carbon layers and generates monolayer graphene. To facilitate graphene growth at low temperature, we used an induction coupled plasma (ICP)-CVD method, employing plasma to decompose the reaction gas, such as C_2H_2 or CH_4, in a low temperature ambient at 750°C. After the reaction gas flow, the samples were cooled to room temperature, and monolayer graphene was then synthesized on the Cu substrate. An XPS analysis was conducted to compare the carbon states of the graphene in order to determine the effects of the transfer process. Additionally, a thermal annealing step was applied after the transfer to enhance the electrical performance, including the mobility and sheet resistance variation.

Results and Discussion

The overall process of the conventional graphene transfer method is summarized in Figure 1. In the transfer process,[10] polymethyl-methacrylate (PMMA) was spin-coated on the graphene layer to protect the graphene from mechanical breakage, and the PMMA/graphene/Cu film was then mechanically peeled off from the SiO_2 substrate. After the peeling step, the Cu substrate, which primarily had been in contact with the SiO_2 substrate, is exposed, and then can be easily etched by a Cu etchant, $FeCl_3$. After Cu etching by floating the film on the surface of the etchant, the remaining PMMA/graphene film adheres the dielectric substrate. Finally, graphene is obtained by removing PMMA using acetone.

In the transfer process described above, chemical and mechanical damages by the metal etching steps are unavoidable. We therefore carried out a XPS analysis after each transfer step to identify the chemical bonding changes of the graphene. Figure 2 shows the XPS results for the carbon and oxygen bonding states on graphene. The mechanically exfoliated graphene on the SiO_2 substrate has C=C and C–OH bonding only (Figure 2a). It is used as a comparison sample against the CVD grown graphene. The CVD grown graphene before the transfer process shows similar results to the mechanically exfoliated sample (Figure 2b). However, an additional oxygen group, O=C–OH, is generated and the amount of C–OH is also increased on the transferred graphene (Figure 2c). These results indicate that graphene suffered chemical bonding damage from the transfer process. Figures 2d and 2e show the results of the graphene/PMMA films after the Cu etching step and the PMMA film, respectively. As Figure 2d indicates, after the Cu etching process, various oxygen bonds such as O=C–OH, C=O, and C–OH are detected in the graphene. However, as shown in Figure 2e, C=O, C–OH, and C=C bonds are also detected on the PMMA, with only O=C–OH bonding being absent. After removal of the PMMA, only O=C–OH bonding remains on the graphene (Figure 2c). Thus, we can conclude that the C=O and C–OH bonds originate from the PMMA and that O=C–OH bonding is generated in the graphene during the Cu etching step. To confirm that graphene is still monolayer after the transfer process, Raman spectroscopy is used. Figure 2f shows a Raman spectrum with a single Lorenzian 2D peak, typical for a monolayer graphene.

To correlate the existence of O=C–OH bonding to degradation of the mobility and doping on the graphene, we measured the mobility, hole concentration and the doping effects before and after the removal of O=C–OH bonding via the following method. The O=C–OH bonding can be removed by a thermal annealing process. We therefore used two approaches: (i) heat-treatment at 350°C in a H_2 or Ar ambient, and (ii) under a high vacuum condition, where the vacuum level is lower than 1×10^{-6}. Figure 3 shows the effects of the thermal annealing processes with various conditions. In all of the thermal annealing processes, the temperature was kept at 350°C for 30 minutes, because higher temperature above 400°C will damage the graphene. In general, thermal annealing processes under high vacuum, Ar, or H_2 ambient can remove O=C–OH bonding on the graphene. Figure 3a shows that a small amount of O=C–OH bonding remains on the graphene after annealing in a high vacuum condition. However, there are no O=C–OH bonding peaks in Figures 3b and 3c, indicating that O=C–OH bonding is completely eliminated by the thermal annealing process with Ar or H_2 ambient. To verify the effects of O=C–OH bonding, hole concentrations of graphene were also measured by Hall effect measurement which is illustrated in Figure 3d. All of the samples have a value of hole concentration around $1.3\times10^{13}/cm^2$. They have sample to sample variations but no relationship with post process annealing was found which means that hole

[z] E-mail: bjcho@ee.kaist.ac.kr

Downloaded 26 Mar 2012 to 143.248.118.104. Redistribution subject to ECS license or copyright; see http://www.ecsdl.org/terms_use.jsp

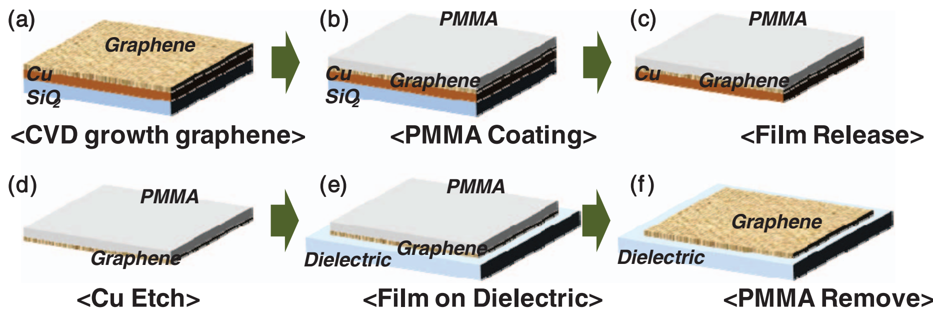

Figure 1. A transfer process for large-scale graphene films grown by CVD. (a) A 4inch wafer-scale graphene grown on Cu/SiO_2 substrate. (b) A PMMA film as a protecting layer spin coated on the graphene. (c) The PMMA/graphene/Cu film mechanically detached from the substrate. (d) Cu etching step using $FeCl_3$, (e) Transfer to a dielectric substrate, and (f) Dissolution of the PMMA film.

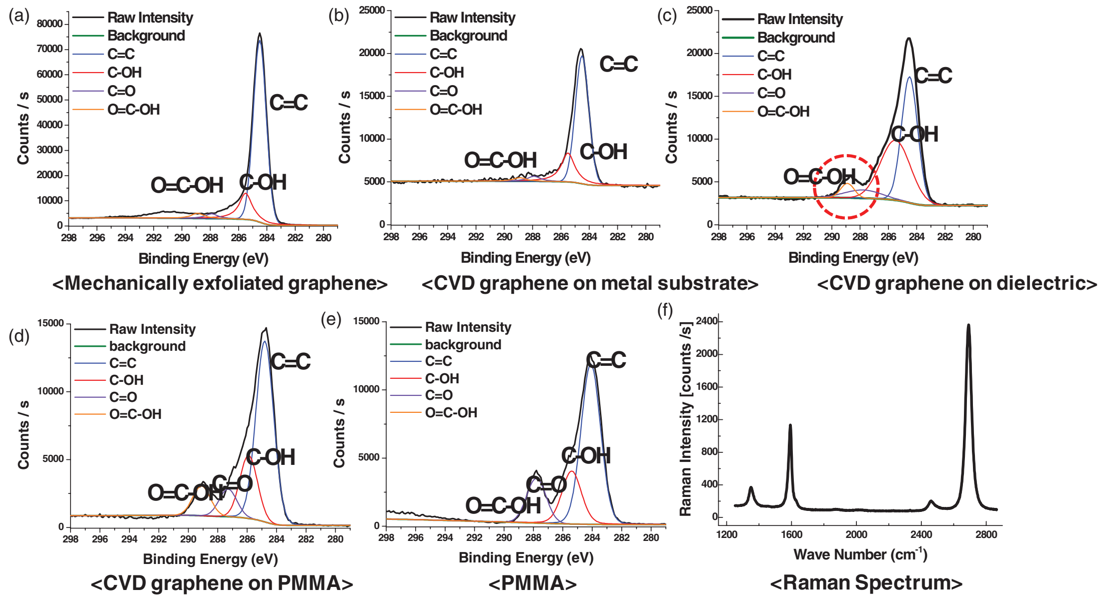

Figure 2. XPS analyzes on the large-scale graphene films grown by CVD after each step. (a) A mechanically exfoliated graphene film on a silicon dioxide substrate for a reference. (b) A monolayer graphene grown by CVD on a Cu substrate and (c) After the transfer to a dielectric substrate. (d) A PMMA/graphene structure after Cu etching step and (e) XPS result of only a PMMA film. (f) A Raman analysis of the graphene grown by CVD after the transfer process.

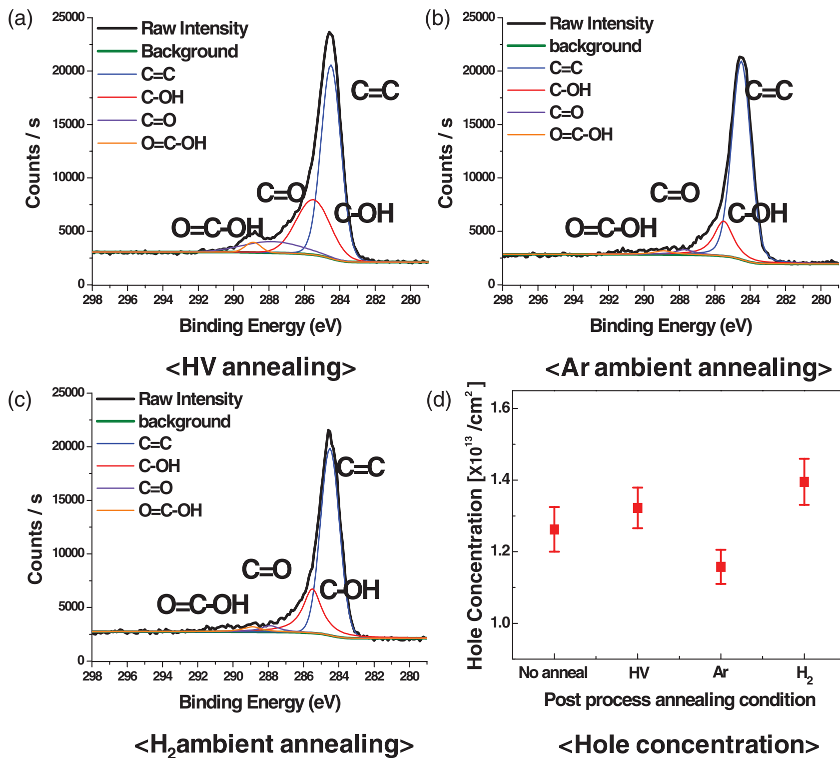

Figure 3. XPS analyzes and variation of hole concentration on large-scale graphene films grown by CVD after the post annealing process; (a) By using a high vacuum condition, (b) By using the Ar ambient, (c) By using the H_2 ambient annealing, and (d) hole concentration depending on post annealing process.

Downloaded 26 Mar 2012 to 143.248.118.104. Redistribution subject to ECS license or copyright; see http://www.ecsdl.org/terms_use.jsp

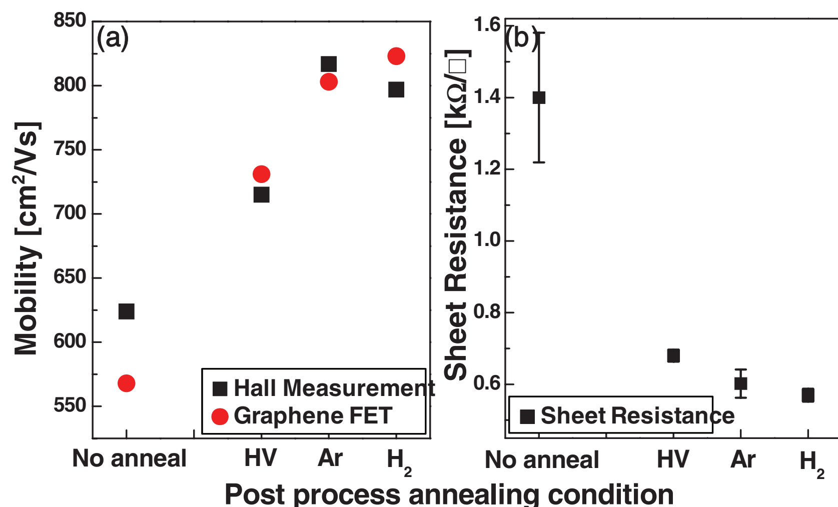

Figure 4. Electrical properties of the transferred graphene after the post annealing process. (a) Mobility variation using a back-gate transistor and the hall-effect measurement, and (b) sheet resistance of the graphene after the various post annealing process.

concentration of graphene cannot be changed by post annealing process. Thus if there are differences in electrical performance among the samples, the O=C–OH bonding in graphene would be the main factor. To evaluate the enhancement of the electrical performance after the annealing process, we employed two methods, Hall effect measurement[11] and electrical measurements from a graphene field effect transistor (FET).[12] In the fabrication of the graphene FET, a p-doped silicon wafer with 100 nm SiO_2 thickness was used with Cr/Au as contact metal. In the Hall-Effect measurement,[11] we extracted the Hall coefficient of the graphene by an applied current in a magnetic field. This approach can be used to extract the carrier mobility and resistivity of graphene. To extract the carrier mobility from the graphene FET,[12] a back gate bias was swept from −20 V to +60 V and the slope of the drain current (I) - gate voltage (V) was used. Figure 4a shows the variation of the carrier mobility depending on the thermal annealing process. The carrier mobility of graphene before the annealing process was nearly 600 cm^2/Vs. When the samples were annealed with Ar or H_2 ambient, the carrier mobility of the graphene was increased to nearly 800 cm^2/Vs. Also, the sheet resistance of the graphene before the annealing process was 1.4 kΩ/□ whereas that of the graphene after the annealing process reached 600 Ω/□ (Figure 4b). The graphene annealed in a high vacuum condition has higher sheet resistance and lower carrier mobility than the Ar or H_2 ambient treated samples. Comparing the results of Figure 3 and Figure 4, we conclude that the enhanced electrical performance after the annealing process can be attributed to the removal of O=C–OH bonding. This can be corroborated by the correlation of the trends from the two different measurement methods, Hall-effect measurement and the graphene FET.

Conclusions

In summary, we determined the critical degradation factor of CVD grown graphene during the transfer process. Although the chemical bonding of the CVD grown graphene before the transfer process is similar to that of mechanically exfoliated graphene, damaged carbon bonding of O=C–OH was generated by the Cu etching step in the transfer process. This bonding can be removed by an annealing process at 350°C in a H_2 or Ar ambient. The removal of O=C–OH bonding improves the carrier mobility of graphene by 30% and decreases the sheet resistance. The results indicate that the formation of O=C–OH bonding must be well controlled during the layer transfer process, especially for electron device application of CVD grown graphene.

Acknowledgments

This work was supported by National Research Foundation of Korea (NRF) Research grant 2010-0029132.

References

1. K. S. Novoselov, A. K. Geim, S. V. Morozov, D. Jiang, M. I. Katsnelson, I. V. Grigorieva, S. V. Dubonos, and A. A. Firsov, *Nature*, **438**, 197 (2005).
2. K. I. Bolotin, K. J. Sikes, Z. Jiang, M. Klima, G. Fudenberg, J. Hone, P. Kim, and H. L. Stormer, *Solid State Commun.*, **146**, 351 (2008).
3. J. S. Bunch, A. M. van der Zande, S. S. Verbridge, I. W. Frank, D. M. Tanenbaum, J. M. Parpia, H. G. Craighead, and P. L. McEuen, *Science*, **315**, 490 (2007).
4. A. Venugopal, J. Chan, X. S. Li, C. W. Magnuson, W. P. Kirk, L. Colombo, R. S. Ruoff, and E. M. Vogel, *J. Appl. Phys.*, **109**, 104511 (2011).
5. K. S. Kim, Y. Zhao, H. Jang, S. Y. Lee, J. M. Kim, K. S. Kim, J.-H. Ahn, P. Kim, J.-Y. Choi, and B. H. Hong, *Nature*, **457**, 706 (2009).
6. X. S. Li, W. W. Cai, J. H. Ahn, S. Kim, J. Nah, D. X. Yang, R. D. Piner, A. Velamakanni, I. Jung, E. Tutuc, S. K. Banerjee, L. Colombo, and R. S. Ruoff, *Science*, **324**, 1312 (2009).
7. X. S. Li, C. W. Magnuson, A. Venugopal, R. M. Tromp, J. B. Hannon, E. M. Vogel, L. Colombo, and R. S. Ruoff, *J. Am. Chem. Soc.*, **133**, 2816 (2011).
8. J. An, E. Voelkl, J. W. Suk, X. S. Li, C. W. Magnuson, L. Fu, P. Tiemeijer, M. Bischoff, B. Freitag, E. Popova, and R. S. Ruoff, *ACS Nano*, **5**, 2433 (2011).
9. X. S. Li, C. W. Magnuson, A. Venugopal, J. An, J. W. Suk, B. Han, M. Borysiak, W. Cai, A. Velamakanni, Y. Zhu, L. Fu, E. M. Vogel, E. Voelkl, L. Colombo, and R. S. Ruoff, *Nano Lett.*, **10**, 4328 (2010).
10. X. S. Li, Y. Zhu, W. W. Cai, M. Borysiak, B. Han, D. Chen, R. D. Piner, L. Colombo, and R. S. Ruoff, *Nano Lett.*, **9**, 4359 (2009).
11. K. S. Novoselov, Z. Jiang, Y. Zhang, S. V. Morozov, H. L. Stormer, U. Zeitler, J. C. Maan, G. S. Boebinger, P. Kim, and A. K. Geim, *Science*, **315**, 1379 (2007).
12. M. C. Lemme, T. J. Echtermeyer, M. Baus, and H. Kurz, *IEEE Electron Dev Lett.*, **28**, 282 (2007).

Downloaded 26 Mar 2012 to 143.248.118.104. Redistribution subject to ECS license or copyright; see http://www.ecsdl.org/terms_use.jsp